Complex shell model representation including antibound states

R. Id Betan*
Departamento de Fisica, Facultad de Ciencias Exactas, Ingeniería Y Agrimensura, Universidad Nacional de Rosario, Avenida Pellegrini 250, 2000 Rosario, Argentina

R. J. Liotta
Royal Institute of Technology (KTH), Alba Nova University Center, SE-10691 Stockholm, Sweden

N. Sandulescu
Institute of Physics and Nuclear Engineering, P.O. Box MG-6, Bucharest-Magurele, Romania, SPhN-DAPNIA, CEA Saclay, F91191 Gif sur Yvette, France

T. Vertse
Institute of Nuclear Research of the Hungarian Academy of Sciences, H-4001 Debrecen, Pf. 51, Hungary, University of Debrecen, Faculty of Information Science, H-4010 Debrecen, Pf. 12, Hungary

R. Wyss
Royal Institute of Technology (KTH), Alba Nova University Center, SE-10691 Stockholm, Sweden
(Received 2 July 2005; published 30 November 2005)

A generalization of the complex shell model formalism is presented that includes antibound states in the basis. These states, together with bound states, Gamow states, and the continuum background, represented by properly chosen scattering waves, form a representation in which all states are treated on the same footing. Two-particle states are evaluated within this formalism, and observable two-particle resonances are defined. The formalism is illustrated in the well-known case of ^{11}Li in its bound ground state and in ^{70}Ca(g.s.), which is also bound. Both cases are found to have a halo structure. These halo structures are described within the generalized complex shell model. We investigated the formation of two-particle resonances in these nuclei, but no evidence of such resonances was found.

DOI: 10.1103/PhysRevC.72.054322 PACS number(s): 21.10.Tg, 23.50.+z, 24.10.Eq

I. INTRODUCTION

One of the most intriguing developments in nuclear physics is the disclosure of antibound states as important building blocks to induce the appearance of halos in exotic nuclei. The explanation of halos as well as the description of the behavior of exotic nuclei, which live a short time and therefore have dynamics governed by processes occuring in the continuum part of the spectrum, requires the introduction of new and powerful models to take into account the complicated interplay among different degrees of freedom that produce weakly bound and resonant states. Such models appeared as soon as the experimental evidence in exotic nuclei provided a variety of features that could not be explained by standard approaches like the shell model using harmonic oscillator representations.

The lively activity that characterizes this field can be attested by the rapid development that is taking place. It would be outside the scope of this paper to assess those models. One of the first reviews is still rather recent [1]. Since then much has been published. In light nuclei a concise but clear account is Ref. [2]. A more comprehensive treatment (including abundant references) can be found in Ref. [3]. The continuum shell model has also been applied for this purpose [4].

Among the attemps to describe the structure of rare nuclei, the complex shell model method (CXSM) [5–7] presents the advantage of incorporating on an equal footing bound single-particle states as well as resonances and the nonresonant continuum. Recently, in a short publication [8], even the elusive antibound states were included in the CXSM basis. Our purpose in this paper is to present in a more extensive fashion the work of Ref. [8]. At the same time the influence of the different ingredients that determine the importance of the antibound state will be appraised by analyzing realistic situations. The formalism is in Sec. II, applications are in Sec. III, and a summary and conclusions are in Sec. IV.

II. FORMALISM

Although the formalism to be used here was given before, we will present it again with some detail for clarity of presentation and also because we will deal with unfamiliar quantities like antibound states and complex probabilities that we would like to clarify from the outset. In addition, we would like to display in the presentation the advantages of working in the complex energy plane, with its implicit loose of familiar quantum mechanical concepts, as compared with standard representations on the real energy axis.

With this in mind we start by pointing out that the study of processes taking part in the continuum part of the

*Electronic address: idbetan@ifir.edu.ar

spectrum may require, by the very nature of the problem, a time-dependent formalism. Therefore the quantum description of the system may become a very hard undertaking. In fact, it may even become an impossible task, since the dynamics of the problem may be very sensitive to the initial conditions and the system can easily precipitate into a chaotic regime. But there are exceptions to this situation. The spectrum corresponding to a system of free particles is a monotonic, continuum function of the energy as determined by the kinetic motion of the particles, and the time-independent Schrödinger equation is suitable to explain this system.

A not so clear situation where time-independent formalisms can be applied occurs even if the particles start to interact with each other under the influence of a central field. Here the continuum may acquire features that depart from the monotonicty of the kinetic energy spectrum. The physical meaning of these structures is that because of the interactions the system remains in a certain configuration for a time, i.e., within an energy interval. In other words, the system is trapped by a barrier erected by the interactions as well as by the centrifugal motion. The structures appearing on the continuum background are the resonances. If the barrier is high enough, for a long time the system will remain in a localized region of space, and the dynamics of the process can be studied within stationary formalisms. The question that one may ask is what is meant by a "long time" or a "barrier high enough." This question is irrelevant in radioactive decay, since measurable mean lives correspond to very narrow resonances. Thus, for the shortest measurable radioactive decay (i.e., the widest measurable resonance) the mean life is at present $T \approx 10^{-12}$ s and the width is, according to the uncertainty relation, $\Gamma = 6.6 \times 10^{-10}$ MeV. Therefore in this time-energy scale the nucleus lives a long time before decaying, and one may assume that the process is stationary. But this is not the case in all processes occurrying in the continuum. In particular, the formation of halos could proceed through wide resonances where even the proper continuum plays a role, as we will see in Sec. III. On the other hand, if the resonance is very wide, the half-life is very short, indicating that the system is not trapped in a barrier for a long time and that the process cannot be considered stationary. One can still try to solve the time-independent Schrödinger equation in this situation to gain insight into the limitations of the problem. Since the system is not trapped by a barrier that is high enough, all or parts of its components will soon depart from the rest. To study this situation in a many-body case is a difficult task. We therefore start from the simplest case, that is, a particle moving in a central field, as Gamow did in the beginning of quantum mechanics [9].

A. Berggren representation

We thus solve the time-independent Schrödinger equation, imposing on the wave function $w_n(r, k_n)$ regularity at the origin and outgoing boundary conditions (the particle departs from the origin); i.e., we require [10]

$$\lim_{r\to 0} w_n(r, k_n) = 0, \quad \lim_{r\to\infty} w_n(r, k_n) = N_n e^{ik_n r}, \tag{1}$$

where k_n is the asymptotic momentum of the state with energy eigenvalue E_n, i.e.,

$$E_n = \frac{\hbar^2}{2\mu} k_n^2. \tag{2}$$

The wave function $w_n(r, k_n)$ thus defined can be considered a generalization of the definition of eigenvectors of the single-particle Schrödinger equation. The eigenvalues E_n can now be complex. Writing

$$k_n = \kappa_n + i\gamma_n, \tag{3}$$

the eigenvectors belonging to those eigenvalues can be classified in four classes, namely (a) bound states, for which $\kappa_n = 0$ and $\gamma_n > 0$; (b) antibound states with $\kappa_n = 0$, $\gamma_n < 0$; (c) decay resonant states with $\kappa_n > 0$, $\gamma_n < 0$; and (d) capture resonant states with $\kappa_n < 0$, $\gamma_n < 0$. From Eq. (1) one sees that only the bound state wave functions do not diverge.

The imaginary part of the energy of the states of class (c) was interpreted by Gamow as minus twice the width of the resonance [9], and therefore these states are usually called Gamow resonances. However, we will make a distinction between real resonances, having physical meaning, and other "resonances" that are generally wide and therefore do not correspond to any particular observable state. To avoid having to distinguish between these different situations anytime we refer to the four classes of outgoing states described above, we will refer to them in general as "poles," since they are the poles of the Green's function [11] and, therefore, of the S matrix.

With the standard definition of a scalar product, only the bound states can be normalized in an infinite interval. Therefore this definition has to be generalized to allow us to use the generalized term "eigenvectors." This can only be done if one uses a biorthogonal basis. As we will see, a consequence of this generalization is that the scalar product between two functions is not the integral of one of the functions times the complex conjugate of the other but rather times the function itself, and one has to apply some regularization method for calculating the resulting integrals. We will perform this task by using the complex rotation method [12].

Berggren found that some of these complex eigenvectors (bound states and decaying resonances) can be used to express the Dirac δ function [13]. We will review the main points of his derivation, since we will come back to it frequently.

One can write the Dirac δ function on the real energy axis, i.e., within a quantum mechanical framework, as [11]

$$\delta(r - r') = \sum_n w_n(r) w_n(r') + \int_0^\infty dE\, u(r, E) u(r', E), \tag{4}$$

where $w_n(r)$ are the bound state wave functions and $u(r, E)$ are scattering states. The integration contour is along the real energy axis. Notice that in the integrand appears the wave function times itself, and not times its complex conjugate, although Eq. (4) is a distribution to be applied on the Hilbert space. This is because for both bound states and scattering states on the real energy axis one can choose the phases such that the wave functions are real.

Berggren extended expression (4) by extending the integration contour to the complex energy plane. Using the

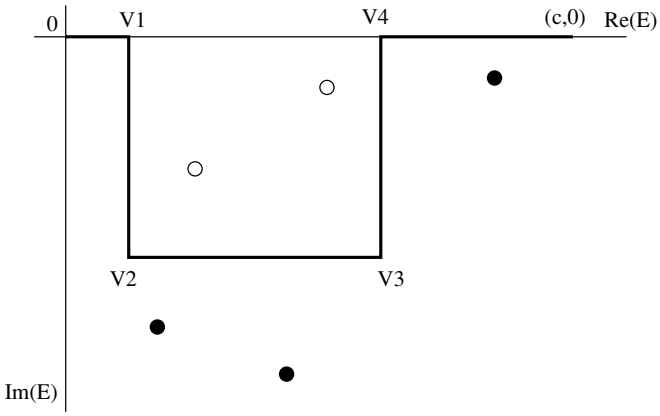

FIG. 1. Integration contour L^+ in the complex energy plane as defined by the vertex points V_i. The open circles represent the Gamow resonances to be included in the sum of Eq. (5), while the solid circles are those that are excluded. The vertex $(c, 0)$ corresponds to the energy cutoff point c.

Cauchy theorem, one gets [13]

$$\delta(r - r') = \sum_n \tilde{w}_n^*(r) w_n(r') + \int_{L^+} dE \tilde{u}^*(r, E) u(r', E), \quad (5)$$

where the sum runs over all the bound states plus the complex poles that lie between the real energy axis and the integration contour L^+, as shown in Fig. 1. This contour may have any form one wishes, but, since it is a topological deformation of the real energy axis, it should be a continuum curve that starts at the origin, i.e., at (0, 0), and ends at infinity, i.e., at $(\infty, 0)$. However, as in any shell model calculation one cuts the basis at a certain maximum energy, which in Fig. 1 is the point $(c, 0)$.

The wave function $\tilde{w}_n(r)$ is the mirror state of $w_n(r, k_n)$, i.e., the solution with $\tilde{k}_n = -k_n^*$. Therefore $\tilde{w}_n^*(r) = w_n(r)$. The same is valid for the scattering state $u(r, E)$. We therefore indeed find that the internal product is the wave function times itself and not times its complex conjugate. This internal product is called the Berggren metric.

The Gamow states enclosed by the contour L^+, plus the bound states and the scattering states on the contour, have been shown to form a complete set of single-particle states (Berggren representation) to describe many-body states in the complex energy plane [14].

Discretizing the integral in Eq. (5), one obtains the set of orthonormal vectors $|\varphi_j\rangle$ forming the Berggren representation. These vectors include the set of bound and Gamow states, i.e., $\varphi_p(r) = \langle r|\varphi_p\rangle = \{w_p(r)\}$, and the discretized scattering states, i.e., $\varphi_p(r) = \langle r|\varphi_p\rangle = \sqrt{h_p} u(r, E_p)$. The quantities E_p and h_p are defined by the procedure that one uses to perform the integration. In the Gaussian method E_p are the Gaussian points and h_p the corresponding weights.

B. Berggren space and resonances

The representation above spans a space called the Berggren space. Since within the metric defining the Berggren space the definition of a scalar product does not include absolute values, one may have probabilities that are complex numbers. We thus find that when forcing the time-dependent process of particles interacting in the continuum to be stationary one has to pay the price of having complex energies and complex probabilities. This is not as weird as it may sound, since we are now dealing with states lying in the complex energy plane, which, in principle, do not have any physical meaning. This is a point that has produced some confusion from the time of the first application of the theory nearly 20 years ago [15]. It is therefore important to clarify the meaning of this feature here, where even another weird feature, namely antibound states, will be introduced.

Let us start by pointing out that the Berggren transformation leading to representation (5) does not change the meaning of the Dirac δ function in any way. In particular, since on the real energy axis the wave functions can be chosen to be real, the results of a continuum shell model many-body calculation of quantities on the real energy axis (like, e.g., sum rules or the energies of bound states) should coincide with the results provided by the same calculation performed by using the Berggren metric with whatever contour one chooses, provided that the resonances enclosed by that contour are also included. This is a very important property that will be used by us to check our results as well as our computer codes. Only for states lying in the complex energy plane will the evaluated quantities be unfamiliar, which is not surprising, since these states lie outside the Hilbert space. Then the question is why one uses the Berggren space or, equivalently, what is the advantage of using the complex energy plane. This is a valid question, which we will therefore answer in some detail.

In the absence of any background, the usual form of the S matrix corresponding to a partial wave (lj) in the neighborhood of an isolated resonance n is

$$\mathcal{S}_{nlj}(E) = \frac{E - E_{nlj}^{(0)} - \frac{i}{2}\Gamma_{nlj}}{E - E_{nlj}^{(0)} + \frac{i}{2}\Gamma_{nlj}} = 1 - \frac{i\Gamma_{nlj}}{E - E_{nlj}^{(0)} + \frac{i}{2}\Gamma_{nlj}}, \quad (6)$$

where $E_{nlj}^{(0)}$ is the position and Γ_{nlj} the width of the resonance. These are real positive numbers.

It is important to point out that Eq. (6) is valid only if the resonance is isolated. This condition is fulfilled for narrow resonances. In this case the residue $\mathcal{R}$ of the S matrix is a pure imaginary number, i.e., $\mathcal{R}_{nlj} = -i\Gamma_{nlj}$, as readily follows from Eq. (6).

The cross section corresponding to the scattering of a particle at an energy close to the isolated resonance takes the form

$$\sigma_{lj}(E) = (2l + 1)\frac{\pi}{k^2} \frac{\Gamma_{lj}^2}{\left(E - E_{lj}^{(0)}\right)^2 + (\Gamma_{lj}/2)^2}. \quad (7)$$

This formula was derived by Breit and Wigner [16] to explain the capture of slow neutrons. It is one of the most successful expressions ever written in quantum physics, as shown by its extensive use in the study of resonances ever since. It was by comparing with experiment that Wigner interpreted the number Γ as the width of the resonance. Since the imaginary part of the S matrix pole is $-\Gamma/2$ [Eq. (6)], this interpretation coincided with the Gamow interpretation of the width. It is often assumed that the value of Γ thus defined is the width of the resonance if it is narrow, i.e., if Γ is small enough.

However, a state having a very small (in absolute value) imaginary part of the energy is not necessarily a physically meaningful resonance. For instance, in the CXSM calculation of two-particle resonances there are states lying very close to the real energy axis that form part of the continuum background because they are induced by basis vectors belonging to the continuum contour [7]. But besides this objection, one may ask what it is meant by "large" and "small" width, even in the case of a pure Gamow pole.

To avoid these objections and to get a more precise definition of a resonance, we note that the condition that the resonance be isolated is equivalent to the requirement that the residues of the S matrix be a pure imaginary number. This criterion was used in Ref. [17] to evaluate partial decay widths corresponding to the emission of neutrons from giant resonances. It was thus found that in only a few cases was the residue of the S matrix a pure imaginary number. Usually that quantity was complex and therefore devoid of any physical meaning. Yet, in some circunstances one can show that the imaginary part of the width thus evaluated (that is, as $\Gamma_{nlj} = 2i\mathcal{R}_{nlj}$) indicates that the lifetime of the resonance is too short and that it can be considered a part of the background [18].

The important conclusion of this discussion is that the imaginary part of the energy, which in some cases can even be evaluated analytically [19], is not in itself related to the width.

A more precise definition of a resonance can be obtained by requiring that the corresponding complex pole posseses some physical attribute. As already pointed out, a measurable resonance corresponds to a process in which the system is trapped inside a barrier for a long time. One can therefore define a resonance according to its degree of localization inside the nuclear volume. This criterion will be very important for identifying the two-particle resonances to be studied in the applications. Thus we will evaluate all resonances that can be built within our Berggren single-particle representation and give physical meaning to the ones with wave functions showing localization properties within the nuclear volume. But it is important to point out that, although this criterion is more accurate for defining a resonance in comparisson with, e.g., one based on the value of the imaginary part of the energy, the very nature of the problem hinders an exact formulation of a criterion to define a resonance in the framework of a time-independent formalism. Therefore even our criterion of defining a resonance according to its localization features has to be considered approximate.

The developing of a resonance depends upon the central mean field as well as the two-body residual interaction acting upon the basis elements. As in any shell model calculation, the interplay among these elements induces the correlated states, which, in our case, include resonances, bound, and antibound states. One thus expects that correlated narrow resonances may be induced not only by bound states and narrow resonances but also by wide resonances, antibound states, and even the continuum itself. The evolution of this complicated process as a function of the interactions as well as the dimension of the basis (including the energy cutoff that defines the representation) can clearly be seen in the complex energy plane, since the location of the complex energies corresponding to the resonances are just points in the two-particle complex plane. This would be very difficult to do on the real energy axis, since here the wave functions corresponding to wide resonances cannot be easily diferentiated from those corresponding to the continuum background. This is an important advantage of using the complex energy plane. We will come back to this point below.

The two-particle shell model equations have the standard form, except the metric, i.e.,

$$(\omega_\alpha - \epsilon_i - \epsilon_j)X(ij;\alpha) = \sum_{k\leqslant l}\langle\tilde{kl};\alpha|V|ij;\alpha\rangle X(kl;\alpha), \quad (8)$$

where α labels two-particle states and i, j, k, l label single-particle states. As in Eq. (5), the tilde denotes mirror states.

In principle the zeroth-order energies $\epsilon_i + \epsilon_j$ would cover the whole two-particle energy plane (since ε is actually a continuous variable), and the correlated state would thus be immersed in a background of uncorrelated states. However, one can avoid this problem by choosing suitable contours [7].

A convenient way of solving Eq. (8) is by using a separable two-body interaction. One thus obtains the dispersion relation [7]

$$-\frac{1}{G_\alpha} = \sum_{i\leqslant j}\frac{f_\alpha^2(ij)}{\omega_\alpha - \epsilon_i - \epsilon_j}, \quad (9)$$

where G_α is the interaction strength and $f_\alpha(ij)$ is the matrix element of the field defining the interaction. We will choose for this field the derivative of the Woods-Saxon potential given by

$$F(r) = \frac{f_0}{1+\exp(r-R')/a'}, \quad (10)$$

i.e., the field f is

$$f(r) = -r\frac{dF(r)}{dr}. \quad (11)$$

This choice of the field defining the two-body interaction differs from the one given in Refs. [5,7], where the function F was the Woods-Saxon potential used to evaluate the single-particle states. The reason for this is that now the central field defining the single-particle states also contains a Gaussian part, as we will see in the Applications (Sec. III). With the present choice of the effective two-body interaction we are able to describe experimental data well, which is the main criterion used in shell model calculations to define the effective force.

The two-particle wave function can be written as

$$X(ij;\alpha) = N_\alpha\frac{f_\alpha(ij)}{\omega_\alpha - \epsilon_i - \epsilon_j}, \quad (12)$$

where N_α is the normalization constant.

This form of the wave function clearly shows the problem one faces if no measure is taken to avoid the continuum background of uncorrelated states. As one chooses more points on the contour (thus improving, in principle, the procedure) the energy denominators corresponding to zeroth-order states close to the energy ω_α diminish and all wave functions tend to a common value, thus making the identification of the correlated resonance impossible.

This possibility of individually identifying the correlated states is another favorable feature of the complex energy plane. On the positive side of the real energy axis (i.e., on the continuum) there is no unique correlated state because the poles of the two-particle Green's function consist only of bound states, which lie on the physical energy sheet, or of resonances located on non physical sheets [20]. Therefore one does not evaluate the energy (i.e., the position) of the resonances on the real energy axis but rather matrix elements of physical operators, like, e.g., transition amplitudes, which increase (in absolute value) close to the resonance energy if the resonance is narrow enough [21,22]. Such limitations do not exist in the complex energy plane. Instead, here one calculates all complex states, but at the end, in order to assign physical meaning to those states as well as to compare with experiment, one chooses the integration contour as the real energy axis. At this point of the calculation the CXSM and standard methods like the continuum shell model coincide. Only complex states showing the resonant features mentioned above (at energies around the real part of the complex energy) will have physical meaning. This is an indication that these states are localized inside the nuclear volume. The wave functions of nonlocalized states are small inside the nuclear volume, and their contribution to the matrix elements of physical operators is also small [23]. This feature will be illustrated below, where we will show localized as well as nonlocalized states.

Usually one chooses the contour of integration L^+ such that it encompasses only Gamow resonances, as in Fig. 1. However, in order to include antibound states, which is a major aim in this paper, one has to choose a generalized contour, which should enclose not only the Gamow resonances but also the antibound states. Since for these states $k_n = -i \mid k_n \mid$, the corresponding energy is real and negative. As we will see, in some circumstances the antibound state has properties similar to the bound state. However, these states are fundamentally different. While the bound state wave function diminishes exponentially at large distances, the outgoing antibound state diverges exponentially.

The antibound states and resonances with $|\gamma_n| > \kappa_n$ were not included in the completeness relations originally suggested by Berggren [13]. This was related to the regularization procedure used in that early work. The first attempt to generalize the completeness by including antibound states and all types of decaying resonances was in a pole RPA approximation [24] in which the complex rotation in the radial distance was used as a regularization method. Later Berggren and Lind also discussed these types of generalized completeness relations [25].

The single-particle states to be used in the applications will, therefore, be determined by the generalized contour shown in Fig. 2. The antibound state in this figure is the open circle on the real energy axis. Notice that the contour lies on the unphysical E sheet, since $\mathrm{Im}(k) < 0$.

We will perform the integration of the scattering states on the continuum contour by using the Gauss method. Assuming that there are N_p poles within the chosen contour and N_g Gaussian points in the integration procedure, the set of generalized basis states consists of $N = N_p + N_g$ elements.

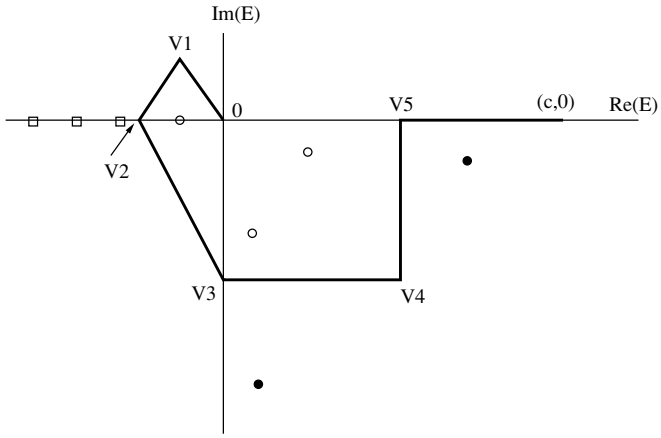

FIG. 2. Generalized integration contour L^+ in the complex energy plane as defined by the vertex points V_i. The open circles represent the antibound states and the Gamow resonances to be included in the Berggren representation, while the solid circles are those that are excluded. The open squares are the bound states, which have to be included independently of the integration contour that is chosen. The vertex $(c, 0)$ corresponds to the energy cutoff point c.

We will order this set such that $n = 1, 2, \ldots, N_p$ labels the poles while $n = N_p + 1, N_p + 2, \ldots, N$ labels the sattering states. The corresponding basis vectors are, with standard notation,

$$\varphi_{nljm}(\vec{r}) = R_{nlj}(r)[\chi_{1/2} Y_l(\hat{r})]_{ljm}. \tag{13}$$

It is important to point out that the Berggren metric affects only the radial part of these functions, while the spin-angular part follows the usual Hilbert metric.

Summarizing this section, we have presented a representation that defines a space (Berggren space) that contains the Hilbert space as a subspace.

The formalism dealing with the many-body applications of the dynamics of a system within the Berggren space is called the complex shell model (CXSM).

The properties of the CXSM are perhaps bizarre, and therefore it is important to clarify some points that we will use in the Applications (Sec. III).

The extension of the Berggren space is defined by the continuum contour. If it is chosen to be the real energy axis, then the resulting CXSM coincides with the shell model. But as soon as the contour departs from the real energy axis, then a new dimension appears in the Berggren space. However, whichever is the contour, the shell model remains a subspace of the CXSM. As a result, all the physical properties evaluated by the standard shell model have to coincide with the corresponding quantities evaluated within the CXSM. In particular, quantities such as transition matrix elements or the angular momentum content of a state corresponding to bound states should be independent of the contour. For a complex state this may not be valid any more, since the state may be outside the Berggren space defined by the chosen contour. For instance (and perhaps obvious), the evaluation of those quantities in complex states by using the real energy axis as a contour would not be possible, since the complex vector is

outside the space spanned by the real energy-axis basis states (i.e., it is outside the Hilbert space).

Concepts like probabilities have no physical meaning for states outside the real energy axis, since they usually become complex quantities. However if the outgoing wave function corresponding to the complex poles shows localization features, then one may be able to consider the state as a resonance, for which the half-life can be defined.

These features will be discussed below.

III. APPLICATIONS

In this Section we will apply the formalism presented above to weakly bound nuclei. The most prominent of these nuclei is ^{11}Li, which we will also treat here but only as an example of the power of the method. In addition, we will show that in the neutron drip-line nucleus ^{70}Ca antibound states play a fundamental role in building the low-energy spectrum.

In all cases the poles as well as the scattering states will be evaluated by using the high-precision piecewise perturbation method [26].

A. Nucleus ^{11}Li

This nucleus has been a testing ground for methods and models invented to describe features associated with weakly bound nuclei, especially halos [1–3]. In the shell model approach one assumes that the odd proton occupying the shell $0p_{3/2}$ is inert and that the low-lying states can be described as two neutrons moving outside the core ^{9}Li. Therefore the ground state of ^{11}Li in this formalism is the 0^+_1 state coupled to the proton state $0p_{3/2}$, which is a pure spectator, providing the angular momentum of the even-odd nucleus but otherwise not contributing in any way to the dynamics leading to the low-lying states. The validity of this approach is justified by the strong correlations between the valence neutrons at large distance, which determine the halo structure of the nucleus as well as the low-energy spectrum [21]. Moreover, disregarding the center of mass motion of the core, as we will do here, is an approximation that was found to work quite well [22].

The core therefore is the nucleus ^{9}Li, corresponding to $N = 6$ neutrons, with the shells $0s_{1/2}$ and $0p_{3/2}$ frozen while the valence shells would be $0p_{1/2}$, $1s_{1/2}$, and perhaps even $0d_{5/2}$ and $0d_{3/2}$. The central field determining these single-particle states is often chosen as a Woods-Saxon potential. However, to reproduce the amount of s-wave content of the ground state wave function in ^{11}Li the depth of the potential was taken to be different for positive- and negative-parity states [8,21,22]. Although with this choice one gets large bindings for the states $0s_{1/2}$ and $0p_{3/2}$ and weakly bound valence shells at the same time, it is an undesirable feature to have to use a central potential that is state dependent. The valence shells are more sensitive to the value of the central potential close to the nuclear surface, indicating that a similar feature would be obtained if one uses a standard Woods-Saxon potential but with an additional central part of short range and large depth. This would ensure a large binding for the states in the core, while the valence shells would be loosely bound. With this in mind, we chose a Woods-Saxon plus Gaussian central potential. The Woods-Saxon potential is defined by the parameters $V_0 = 39.97$ MeV, $V_0^{so} = 19.43$ MeV, $r_0 = r_0^{so} = 1.27$ fm, $a = a^{so} = 0.67$ fm, while the Gaussian potential is $V(\text{Gauss}) = -\text{V}_\text{g} \exp[-(\text{r}/\text{a}_\text{g})^2]$ with $V_g = 663$ MeV and $a_g = 0.26$ fm. The resulting single-particle states are given in Table I.

TABLE I. Single-particle states used in the calculation of the two-neutron states in ^{11}Li. The energy E_n and the wave number k_n are related as in Eq. (2). The k_n value corresponding to the state $1s_{1/2}$ shows that this is an antibound state.

State	E_n (MeV)	k_n (fm^{-1})
$0s_{1/2}$	(−20.61, 0)	(0, 0.945)
$0p_{3/2}$	(−4.525, 0)	(0, 0.443)
$1s_{1/2}$	(−0.025, 0)	(0, −0.033)
$0p_{1/2}$	(0.240, −0.064)	(0.103, −0.013)
$0d_{5/2}$	(4.334, −1.638)	(0.441, −0.081)
$0d_{3/2}$	(6.396, −9.898)	(0.628, −0.342)

One indeed sees that the shells $0s_{1/2}$ and $0p_{3/2}$ are deeply bound while the shell $1s_{1/2}$ lies close to threshold, but as an antibound state, as required by experimental evidence [27], and the shell $0p_{1/2}$ appears as a resonance at 240 keV and a width of 128 keV, as also required by experiment [28]. These two unbound states are the valence shells. They will determine the bound ground state of ^{11}Li, giving to the three-body system consisting of the core, i.e., ^{9}Li, and the two neutrons its Borromean character [1].

We are assigning the features of a bound state to the shell $1s_{1/2}$ by labeling it with the principal quantum number $n = 1$. This indicates that it has only one node (excluding the origin), although it is an antibound state. To show that this is indeed the case *inside* the nuclear volume, i.e., that this complex state is localized, we have plotted the radial part $R_p(r)$ (with $p \equiv 1s_{1/2}$) of the corresponding wave function in Fig. 3. In this figure we also plotted the wave function corresponding to the equivalent bound state, i.e., with the same negative energy. To obtain the same energy as before but now bound (instead of antibound), we changed the depth of the Woods-Saxon potential to the value $V_0 = 42.97$ MeV (instead of $V_0 = 39.97$ MeV). The rest of the parameters defining the mean field (including the Gaussian part) are the same as before.

With the usual definition of the nuclear radius, i.e., $R = r_0 A^{1/3}$, $r_0 = 1.25$ fm, and $A = 10$, one gets $R = 2.69$ fm, but in this neutron $l = 0$ case there is not any barrier, and the states lie so near the continuum threshold that the bound wave function extends far beyond the nuclear radius. This feature motivated the assumption of a weakly bound $1s_{1/2}$ state in ^{10}Li when the halo structure of ^{11}Li was discovered. However, although great experimental efforts were made searching for such a state, no trace of it was ever found [1]. Finally, the $n+^{9}$Li system was measured to have a large and negative scattering length (-17 fm), which prompted the realization that the state $1s_{1/2}$ indeed exists here at low energy but actually as an antibound (or virtual) state [27].

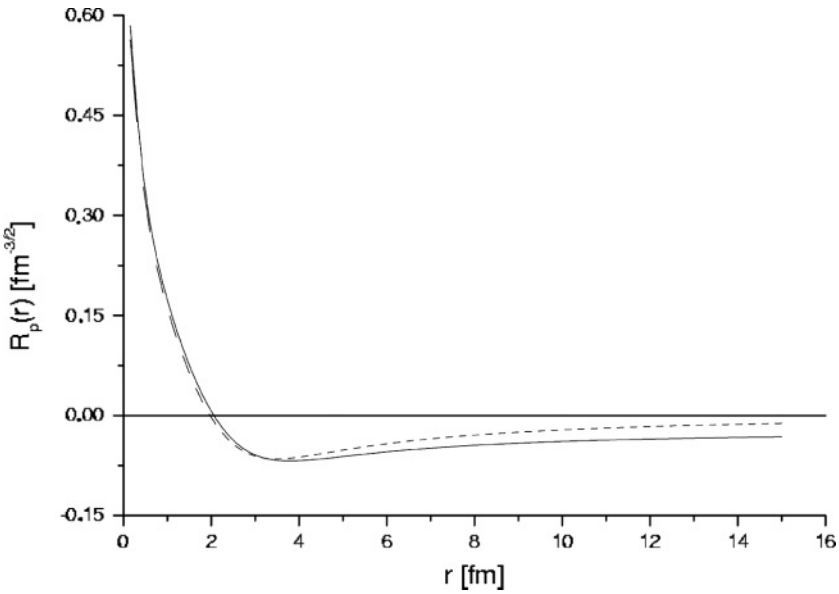

FIG. 3. Radial wave function $R_{1s_{1/2}}(r)$ [Eq. (13)] corresponding to the bound (dashed curve) and antibound (solid curve) states in ^{10}Li at $(-0.025, 0)$ MeV. The bound state was obtained by changing the depth of the Woods-Saxon potential, as explained in the text. The bound (antibound) wave function is purely real (imaginary).

In fact there is a similarity between bound and antibound states lying close to the continuum threshold. One sees in Fig. 3 that for these states the wave functions inside the nucleus are practically identical. They depart from each other only at large distances. Here the antibound wave function increases, eventually diverging. As mentioned above, the CXSM takes care of this divergence by regularizing all integrals, using the complex rotation.

The localization of the antibound state can also be deduced from the behavior of the corresponding scattering wave function on the real energy axis. At the energy $E = \hbar^2 k^2/2\mu$ (k real and positive) close to a bound or antibound state lying at a energy E_0 near threshold the scattering wave function can be written as [29],

$$R_l(kr) \approx \sqrt{\frac{2k|k_0|}{k^2 + |k_0|^2}}\, R_l(|k_0|r), \tag{14}$$

where $R_l(|k_0|r)$ is the scattering function at *positive* energy $|E_0|$, although the wave numbers for the bound or antibound state are purely imaginary, i.e., $k_0 = \pm i|k_0|$, respectively. That is, the energy values for these states are negative, $E_0 < 0$, but they lie on different energy sheets.

Expression (14) shows that close to threshold the radial shape of the scattering wave functions is independent of the energy E and that the wave function depends on E (k) only in its magnitude through the square root factor. This factor has its maximum at $k = |k_0|$, and therefore the large matrix elements in an energy region close to E_0 are induced by the S-matrix pole at imaginary k_0. In particular, as seen from Eq. (12), the two-body wave function in that energy region will be large on the real energy axis (i.e., within the continuum shell model). As we will see, this feature explains the large $l = 0$ content of the ^{11}Li(g.s.) wave function. The remarkable point in this argument is that it does not matter whether the pole at $E_0 < 0$ corresponds to a bound or to an antibound state. Only the absolute value of E_0 is relevant, and the effect is the same for both types of states, as expected from Fig. 3.

One should not take the similarity between bound and antibound states too far. To appraise this we notice that in the presence of a high barrier a bound state lying near the continuum threshold becomes a narrow Gamow resonance if one changes the central potential adequately, as we did above [23]. The imaginary part of the Gamow wave function thus obtained is small, while the real part is very much like the bound state in a range up to about twice the nuclear radius. Moreover, the Gamow wave functions of all narrow resonances, not only those lying near the continuum threshold, have negligible imaginary parts and real parts that are very similar, within the nuclear range as above, to the ones provided by a standard harmonic oscillator potential [23]. This feature explains why harmonic oscillator representations have been very successful in describing observable cluster decays, i.e., very narrow resonances [30]. But we want to stress, once again, that in general it is not the imaginary part of the energy that is a proper measure of the width of a resonance but rather the localization of the corresponding wave function. As we have already discussed, the relation between $\mathrm{Im}(E_n)$ and Γ_n is valid only if the width thus obtained coincides with the Breit-Wigner definition, i.e., if it satisfies Eq. (6). This occurs if the resonance is isolated, in which case the wave function is localized, as occurs with narrow Gamow resonances.

The limitations of the definition of the width as twice $-\mathrm{Im}(E_n)$ can clearly be seen by trying to apply it to our weakly antibound $1s_{1/2}$ state, which cannot have any relation with physically meaningful Gamow resonances, since there is no barrier to trap the system within the nuclear region [yet, there are Gamow-type $s_{1/2}$ poles at bizarre energies, like very large values of $-\mathrm{Im}(E_n)$]. Even more, no antibound state can be related to Gamow resonances, since the energy is purely real. That is, one cannot recognize the physical meaning of the antibound state by analyzing its properties

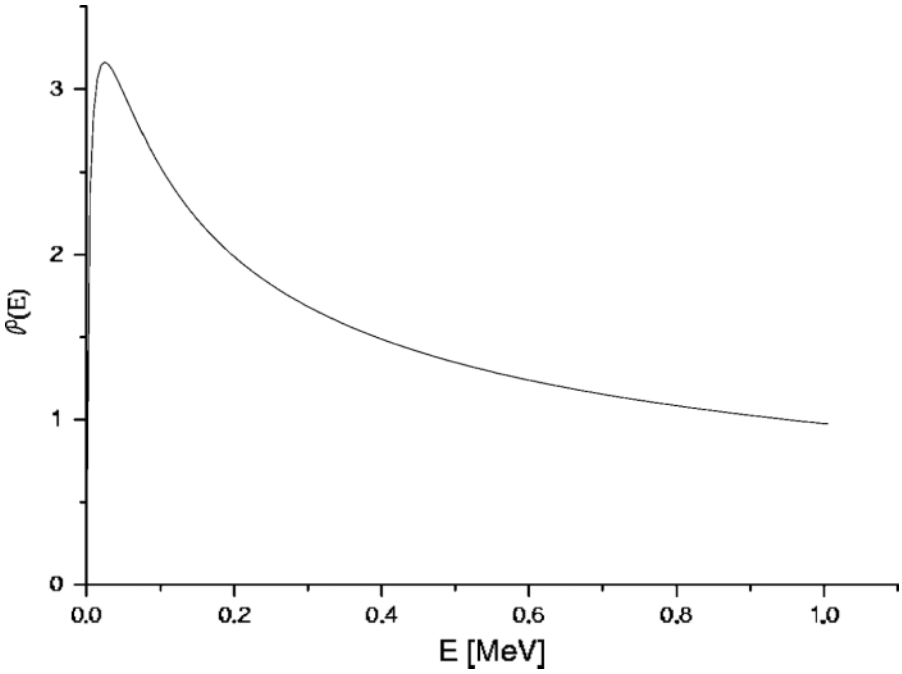

FIG. 4. Function $\mathcal{P}(E)/A$, Eq. (15), corresponding to the antibound state at energy $E_0 = -0.025$ MeV of Fig. 3.

in the complex energy plane, since here quantum mechanics is not valid. Instead one has to evaluate meaningful transitions *on the real energy axis*. Thus, the probability $\mathcal{P}(E)$ that the neutron escapes from the nucleus carrying a kinetic energy E is proportional to $|R_l(kr)|^2$, which vanishes at large radius for bound states. Instead, for antibound states one gets, from Eq. (14),

$$\mathcal{P}(E) = A\frac{\sqrt{E}}{E + E_0}, \tag{15}$$

where A is an energy-independent quantity. As seen in Fig. 4, this probability looks like the one corresponding to the decay from a state at *positive* energy $|E_0|$. That is, in a decaying process the antibound state does not behave as a bound state but rather, again, as a Gamow resonance but having a width unrelated to the energy.

The conclusion of this discussion is that poles may have physical meaning *only* if the corresponding wave function is localized. As an illustration of a nonlocalized pole we show in Fig. 5 the wave function corresponding to the resonance $0d_{3/2}$ of Table I. This state is so wide that it may be considered part of the continuum background, since in a region surrounding the nuclear core its value is very small. As for the antibound state discussed previously the wave function increases with distance, but the difference from that case is that now the increase is huge even at a rather short distance. This state cannot be expected to have any physical significance. Yet we will include it in the generalized Berggren basis. In fact, one of the reasons that we apply high-presicion methods [26] in our calculations is to avoid numerical errors that would otherwise appear when states with large imaginary parts have to be considered.

A state that will be fundamental to build the low-lying spectrum of ^{11}Li is the Gamow pole $0p_{1/2}$, and, therefore, we show the corresponding wave function in Fig. 6. The imaginary part of the energy is in this case not very small in comparisson with the corresponding real part. Yet the wave function shows clear localization features. This state can be considered a resonance.

One does not need to use the same integration contour for all the single-particle states, since within the Berggren metric basis states are independent of one another. It is therefore convenient to use in each case a contour adapted to the position of the poles. In our case only for the antibound state is it necessary to have a contour that lies outside the fourth quadrant in the complex energy plane, such as the one in Fig. 2. For the other partial waves corresponding to the poles of Table I we will use a contour like the one in Fig. 1. Moreover, in each segment $V_i - V_{i-1}$ [with $i > 0$ and $V_0 = (0, 0)$] we choose a different number of points according to how near a pole is to the segment. The values of the vertices V_i and the number of points N_i between adjacent vertices defining our Berggren basis is given in Table II. The value of N_i is the smallest number of Gaussian points that provides a convergence of the results of at least five digits in the energies and at least four digits in the wave functions.

The valence poles plus the scattering states thus defined constitute our generalized single-particle Berggren basis.

The two-particle basis is built from the single-particle states as usual. To evaluate the two-body energies and corresponding wave functions, one has to solve dispersion relation (9). To determine the strength G_α we will use the standard procedure of adjusting its value to fit the lowest energy of the two-particle state carrying angular momentum λ_α (and parity $(-1)^{\lambda_\alpha}$, since the force is separable).

The only two-neutron positive-parity state for which there is any experimental data in ^{11}Li is the ground state, i.e., $\lambda_\alpha = 0$ (although due to the presence of the proton the real spin of ^{11}Li(g.s.) is $3/2^-$). The corresponding experimental energy is $\omega_{n_\alpha=1,\lambda_\alpha=0} \approx -0.295$ MeV^2.

TABLE II. Vertices V_i (in MeV) in the integration contours of Fig. 1, corresponding to all partial waves with values of (l, j), such as those in the states of Table I except for the partial wave $s_{1/2}$, for which the contour shown in Fig. 2 was used. N_i is the number of Gaussian integration points in the segment between the vertices V_i and V_{i-1}. The point V_0 (not shown in the table or figures) is the origin, i.e., $V_0 = (0, 0)$. The energy cutoff point is $(c, 0) = 10$ MeV, and the number of Gaussian points between the last vertex and the cutoff point $(c, 0)$ is four in all cases.

Partial Wave	V_1	N_1	V_2	N_2	V_3	N_3	V_4	N_4	V_5	N_5
$s_{1/2}$	$(-0.025, 0.1)$	10	$(-0.050, 0)$	10	$(0, -0.07)$	20	$(3, -0.7)$	6	$(3, 0)$	2
$p_{3/2}$	$(0.1, 0)$	2	$(0.1, -0.7)$	4	$(3, -0.7)$	4	$(3, 0)$	4	—	—
$p_{1/2}$	$(0.1, 0)$	2	$(0.1, -0.7)$	6	$(3, -0.7)$	10	$(3, 0)$	6	—	—
$d_{5/2}$	$(3.5, 0)$	4	$(3.5, -3)$	4	$(5, -3)$	4	$(5, 0)$	4	—	—
$d_{3/2}$	$(5, 0)$	4	$(5, -10.7)$	4	$(8, -10.7)$	4	$(8, 0)$	4	—	—

The short range and attractive character of the residual nuclear interaction causes the lowest 0^+ state to lie below the lowest two-particle configuration. Therefore the vertex $V_2 = (a, 0)$ in Fig. 2 has to fulfill the condition $\omega_{0_1^+} < 2a$. This restricts the position of the vertex V_2 to the range -0.1 MeV $< a < -0.025$ MeV. As is seen in Table II, we use $V_2 = (-0.050, 0)$ MeV, which is very close to the energy of the antibound state. This is not an optimal situation, since close to a pole the scattering waves increase rapidly as the energy approaches the pole. In fact, one of the advantages of using representation (5) for the Dirac δ function is to avoid the numerical difficulties that one encounters when integrating on the real energy axis in the presence of very narrow resonances. These difficulties can be overcome by choosing an integration countour lying far enough from the resonance energy [31]. In our case the contour has to be near the pole, and therefore we had to use many integrations points around the antibound state. This explains the relatively large values of N_1, N_2, and N_3 corresponding to the partial wave $s_{1/2}$ in Table II.

Another undesirable feature of this situation is that the two-particle configurations corresponding to the scattering states may acquire values that are very large [according to Eq. (12)] and therefore unfamiliar. But this is not a problem in itself, since the wave-function components in the complex energy plane depend on the contour that one uses. It is worthwhile to point out again that the results have physical meaning only when evaluating quantities defined on the real energy axis, such as, for instance, the energies of bound states or the angular momentum content of the two-particle wave functions of those bound states. The ground state of ^{11}Li lies at about -295 keV, as mentioned above, and the angular momentum content is about 60% s states and 40% p states, although some small components of other angular momenta are not excluded [2].

Notice that for bound states the angular momentum content A_l does not depend upon the contour because it is a sum over all basis states. Thus, for states with angular momentum $\lambda_\alpha = 0$, it is

$$A_l = \sum_{nn'l' \neq lj} X(nl'j, n'l'j; \alpha)^2, \tag{16}$$

which is a real number if the state α is bound and complex otherwise, since the real energy axis is excluded as a contour

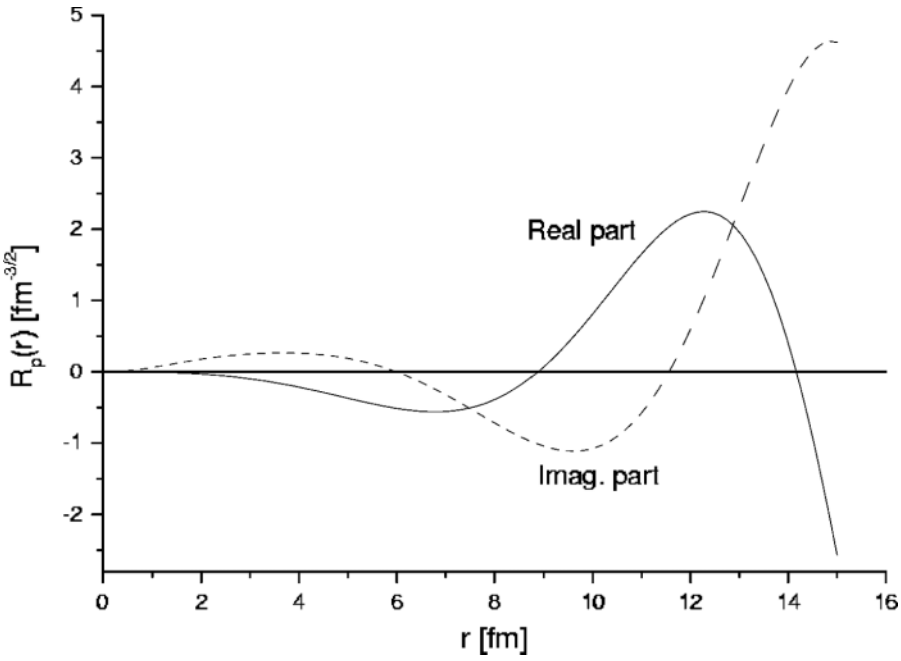

FIG. 5. Radial wave function $R_{0d_{3/2}}(r)$ corresponding to the resonance of Table I. Notice the large values of the wave function here in comparisson with those in Fig. 3.

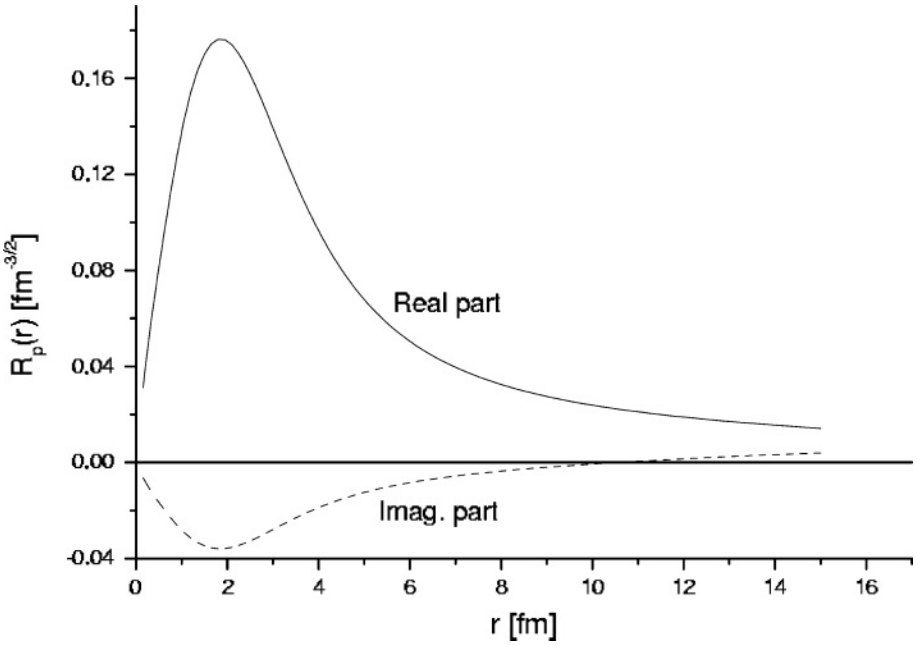

FIG. 6. Radial wave function $R_{0p_{1/2}}(r)$ corresponding to the single-particle state in Table I.

to describe complex states. This also implies that A_l (as well as all physical quantities corresponding to resonances which are not isolated) may depend on the contour if this contour defines a Berggren space that does not fully contain the resonance. However, owing to the normalization of the state, it is $\sum_l A_l = 1$ in all cases.

The imaginary part of A_l may give a measure of how significant (isolated) is the complex state. If $|\mathrm{Im}(A_l)|$ is large, then the state may be considered a part of the two-particle continuum background. Again, here it is not very clear what is meant by large, and it would be more convenient to answer this question by looking at the localization of the corresponding wave function, as we will do below.

The property that A_l for bound states do not depend upon the contour has been used by us as an important test for checking our computer codes.

The energy of ^{11}Li(g.s.) will be fitted to adjust the strength G_α of the separable interaction. Therefore it is G_α that should remain the same and a real number (since the Hamiltonian is Hermitian) as one changes the contour.

Using for the field [Eq. (11)] the parameters $f_0 = 10$, $R' = 4.5$ fm, and $a' = 1.5$ fm, we evaluated within the generalized Berggren basis defined above the strength from Eq. (9) to obtain the value $G_0 = 0.1659$ MeV. Using as a contour the real energy axis, we obtained the same value, confirming the formalism as well as the precision of our computer codes.

The dispersion relation has as many solutions as the dimension of the two-particle basis. The overwhelming majority of these solutions form part of the continuum background. These continuum states are easy to recognize because they feel the interaction very weakly and therefore they lie very close to their zeroth order energy, i.e., they are ordered according to the lines defining the contour. For illustrations of this feature see Ref. [7]. The physically meaningful states are localized, and, therefore, one expects that the main wave-function configurations of the relevant two-particle states should correspond to bound states or resonances. One indeed finds this feature in the main wave-function components of the ground state (i.e., 0^+_1) at -0.295 MeV and in a state at (0.274, -0.247) MeV (0^+_2), which may be a resonance. The largest of those components are

$$|0^+_1\rangle = (1.79, 0)|(1s_{1/2})^2\rangle + (0.15, 1.02)|(1s_{1/2}c_1)\rangle + (0.03, 0.98)|(1s_{1/2}c_2)\rangle,$$

$$|0^+_2\rangle = (0.70, 0.12)|(0p_{1/2})^2\rangle + (-0.50, -0.08)|(0p_{1/2}c_3)\rangle + (0.36, -0.15)|(0p_{1/2}c_4)\rangle,$$

where c_i are states belonging to the continuum contour, i.e., they are scattering waves with angular momenta (l, j) and energies ϵ_i (in MeV) given by

$$|c_1\rangle = |l = 0, \quad j = 1/2, \quad \epsilon_1 = (-0.048, -0.031)\rangle,$$
$$|c_2\rangle = |l = 0, \quad j = 1/2, \quad \epsilon_2 = (-0.046, -0.056)\rangle,$$
$$|c_3\rangle = |l = 1, \quad j = 1/2, \quad \epsilon_3 = (0, -0.266)\rangle,$$
$$|c_4\rangle = |l = 1, \quad j = 1/2, \quad \epsilon_4 = (0, -0.119)\rangle.$$

These continuum states are important in the description of our relevant 0^+ levels because the zeroth-order energies of the corresponding two-particle basis states are very close to the correlated energies. However, the CXSM wave-function components depend on the contour that one chooses, and, therefore, they have physical meaning only if the contour coincides with the real energy axis, as in the continuum shell model. This feature is valid even if the state is bound, although in this case the wave function itself does not depend on the contour, and it has the normal physical meaning of quantum mechanics, as we will see below.

Since the components of the CXSM wave function are not well-defined quantities, it may seem unreasonable to probe

features like localization by analyzing such components, as we did above. However, we have found that physically relevant states always have wave functions with main components consisting of bound or resonant single-particle states, independently of the contour one chooses. In our case, the quantity that has a physical (i.e., quantum mechanical) significance is the angular momentum content A_l, Eq. (16). We found that for the ground state A_l is, in percentage, 49% s states, 47% p states, and 4% d states, in agreement with experiment.

Although for bound states A_l is real, its components may be complex, contour dependent, and have very large absolute values. For instance, in ^{11}Li(g.s.) the contribution of the pole-pole component $|(1s_{1/2})^2\rangle$ is (3.218, 0.004), while the pole-continuum components $|1s_{1/2}c_i\rangle$, where c_i is an s wave on the contour, add up to (−8.473, −0.009) and the continuum-continuum components $|c_i c_j\rangle$ to (5.746, 0.005). The corresponding values for the p waves is (0.598, −0.202) for the pole-pole component $|(1p_{1/2})^2\rangle$, (−0.146, 0.218) for the pole-continuum components $|1p_{1/2}c_i\rangle$, and (0.001, −0.016) for the continuum-continuum components. The $p_{3/2}$, $d_{3/2}$, and $d_{5/2}$ contribution adds up to a total of (0.060, 0). The total sum is the value 0.49 for the s waves, 0.47 for the p waves, and 0.04 for the d waves, as quoted above. That is, the total sum is real and represents a probability, while the partial components have no meaning and are contour dependent. Notice that this is valid even for the pole-pole component, since its value is proportional to the wave function amplitude X, which depends on the contour through the normalization constant [see Eq. (12)].

In a calculation performed on the real energy axis there are neither pole-pole nor pole-continuum contributions (since there is no bound single-particle state in this case), and all partial contributions are continuum-continuum components that are probabilities; i.e., they are real, positive, and less than or equal to unity. These values coincide with the percentages of A_l given above, once again confirming the reliability of our codes.

For the 0_2^+ state all partial contributions to A_l are complex, although they have to add up to unity owing to the normalization of the CXSM wave function. One thus obtains that A_l is (13, −10)% s states and (87, 10)% p states, indicating that this resonance is mainly built on the $0p_{1/2}$ single-particle resonance.

It is interesting to see how the mixing among the various components of the angular momentum content evolves as the strength of the interaction increases from the zeroth-order value where the states are indeed given by the poles; i.e., for $G = 0$ it is 100% s states for 0_1^+ and 100% p states for 0_2^+. In Table III we present the evolution of these values, as well as the energies of the states, as a function of the strength G.

Looking at the imaginary values of these quantities as well as at the energy of the predicted 0_2^+ state [i.e., (0.274, −0.247) MeV], which is large; one may doubt whether this state is indeed a resonance and therefore whether it could be detected experimentally. To decide this we will analyze its localization properties. But first we have to learn which are the features that determine such localization in this weakly bound nucleus. This can be done by studing the two-particle wave function of the bound ground state. This would help us to decide whether the state 0_2^+ is indeed a resonance by comparing the properties of its wave function with those of the ground state. A convenient way of doing this is by exploiting the clustering features of the ground state wave function in the singlet ($S = 0$) component [32]. We will call $S(r)$ this singlet part of the wave function. Its expression can be found in Ref. [32].

Because of the two-neutron clustering, one can recognize whether the center of mass of the two-neutron system remains inside the nuclear core by analyzing $S(r)$ in some direction, for instance in the x direction. That is, we will choose $r = r_1 = r_2$, where $\vec{r}_i = (r_i, \theta_i, \phi_i)$ is the coordinate of the particle i with $\theta_i = \pi/2, \phi_i = 0$. Notice that this direction is irrelevant, since the system is spherically symmetric.

In Fig. 7 we show the function $S(r)$ corresponding to the ground state of ^{11}Li. One sees that inside the nucleus the wave function of the two valence particles is highest and the corresponding imaginary part smallest, indicating that there is a localization. Since this is the quantum mechanical wave function corresponding to the bound system, its value should not only be independent of the contour but should also represent a probability amplitude. Therefore the small imaginary part that appears at long distance has to be considered a limitation of the calculation. One also sees that this wave function extends far outside the nucleus, as expected, since this is the feature that causes the halo. Yet, one may think that the imaginary part as well as the large value of the real part at large distances is an effect of the diverging character of the complex wave functions in the generalized Berggren basis. To be sure that this is not the case, and considering

TABLE III. Energies E and angular momentum content $A_l \times 100$, Eq. (16), for the angular momenta $l = 0, 1, 2$ (s, p, d), corresponding to the states 0_1^+ and 0_2^+ in ^{11}Li as a function of the interaction strength G. The strength fitting the available experimental data is $G_0 = 0.1659$ MeV.

G (MeV)	0_1^+				0_2^+			
	E MeV	s	p	d	E (MeV)	s	p	d
0.01	−0.061	100	0	0	(0.466, −0.117)	0	(100, 0)	0
0.05	−0.091	100	0	0	(0.388, −0.089)	(−4, 0)	(104, 0)	0
0.09	−0.092	100	0	0	(0.292, −0.144)	(−14, −12)	(114, 12)	0
0.13	−0.102	99	1	0	(0.261, −0.224)	(14, −9)	(86, 9)	0
0.17	−0.328	48	47	5	(0.271, −0.276)	(17, −4)	(83, 4)	0

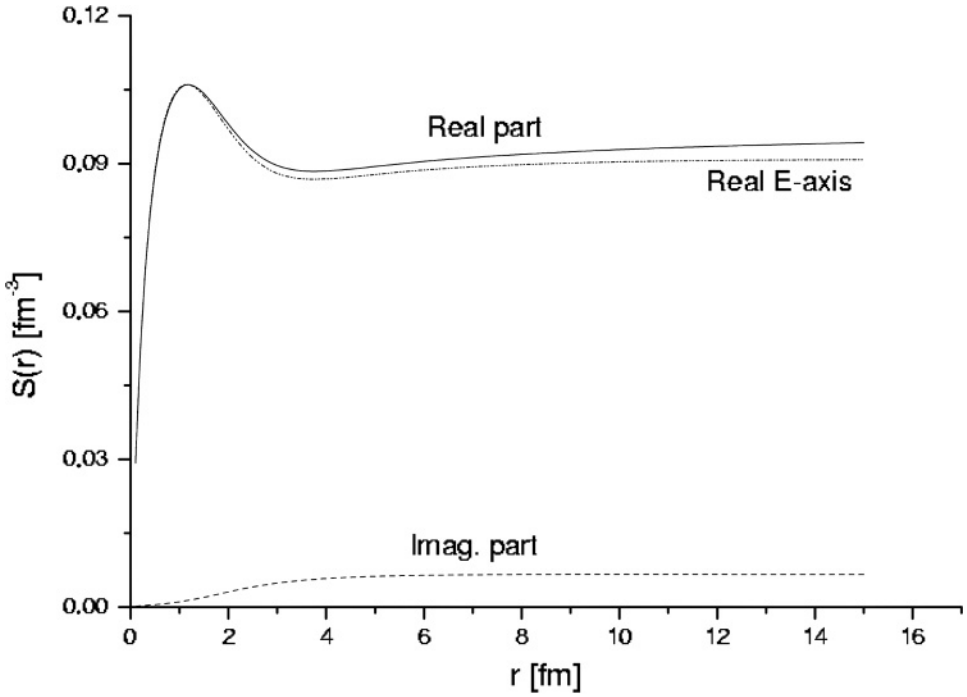

FIG. 7. Two-particle radial wave function $S(r)$ corresponding to the singlet component of the ground state of ^{11}Li evaluated by using the generalized Berggren representation. The dashed curve is the same wave function but using as a representation the real energy axis, i.e., calculated within the continuum shell model framework.

that this wave function has a physical meaning, we calculated it again but using the real energy axis as a representation. As seen in the Fig. 7, we found that the wave function thus calculated is virtually the same as the one using the generalized Berggren representation. As with the imaginary part, there are small differences at large distances, and this has to be attributed to computational limitations that make it difficult to treat the diverging character of the single-particle states exactly.

As a final comment, it has to be noted that, although the two-particle wave function extends far in space (a feature that is known, see e.g., Fig. 1 of Ref. [21]), the mean square radius of the nucleus is not excessively large, since this quantity is strongly influenced by the particles in the core, including the three protons [21]. The extension of the wave function corresponding to the valence particles provides a tiny contribution to the total wave function of the nucleus, which is the reason that the density of the halo is low.

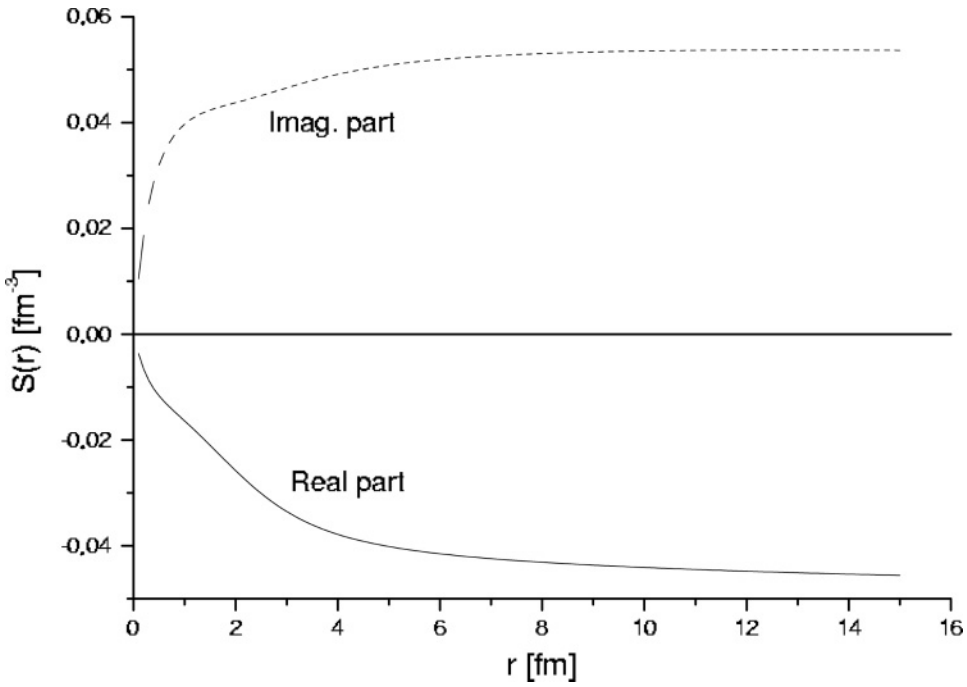

FIG. 8. Two-particle radial wave function $S(r)$ corresponding to the singlet component of the state $^{11}\mathrm{Li}(0_2^+)$ evaluated by using the generalized Berggren representation.

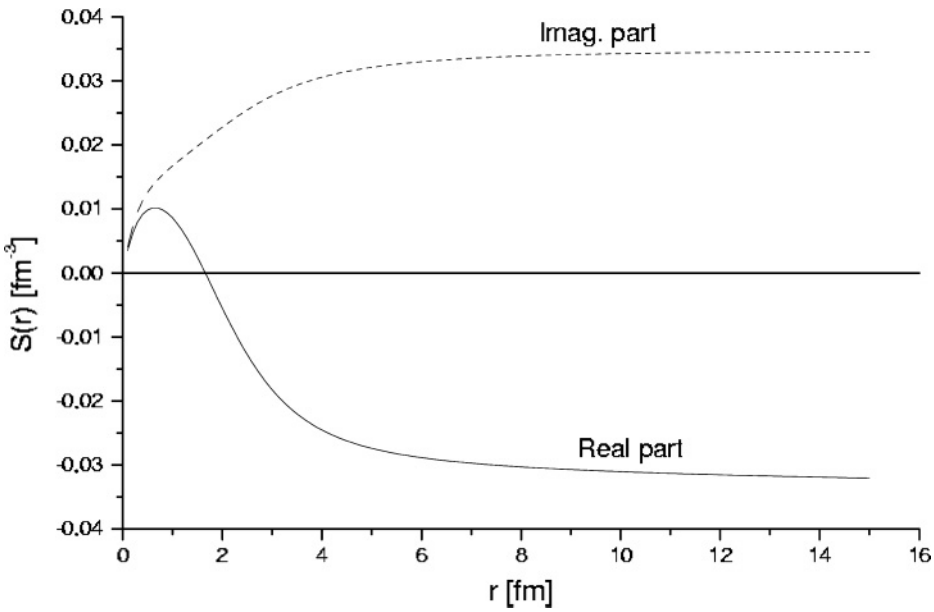

FIG. 9. Two-particle radial wave function $S(r)$ corresponding to the singlet component of the state $^{11}\mathrm{Li}(0_2^+)$ evaluated by using the generalized Berggren representation with a $G = 0.05$ MeV interaction.

We are now in a position to analyze the wave function of the 0_2^+ state. We thus plotted in Fig. 8 the singlet function $S(r)$ for this state. We see that now the wave function does not show any localization feature inside the nucleus. Perhaps even worse, the imaginary part is very large, thus providing a large imaginary part of the probability if it were to be assigned a quantum mechanical meaning. This state is not a resonance, and therefore it is not surprising that it has not been observed.

The narrowest 0_2^+ state in Table III corresponds to $G = 0.05$ MeV. One may thus learn from this case whether its small imaginary part of the energy implies that it is localized. We thus plotted in Fig. 9 the corresponding function $S(r)$. One sees that something very strange happens. While the real part of the wave function shows localization, the imaginary part does not. Again, the criterion of defining a resonance according to its localization features shows that this is neither a physically meaningful state. Yet, it is remarkable that as G increases this state first becomes narrower, and then, just after $G = 0.05$ MeV in Table III, its width increases rather fast. This indicates that at this value of G there is a mechanism that moves the state down in the complex energy plane. To examine this feature we show in Table IV the dependence of the angular momentum content for each partial wave on G. We show only the s and p components, since the other angular momenta play no role here. One sees in Table IV that the mixing between these components is not as strong as the mixing between the pole-pole $|(1p_{1/2})^2\rangle$ component and the pole-continuum components. It is also conspicuous that the continuum-continuum $l = 1$ partial waves have virtually no influence. One therefore can conclude that the reason that the state does not become narrower as the interaction increases is that the coupling of the single-particle resonance to the continuum becomes stronger with an stronger interaction, and, as a result, the two-particle state is itself pushed toward the continuum. At no value of G is the two-particle system in the 0_2^+ complex state trapped by the interaction inside the nucleus, and the state never becomes a resonance.

Finally, it is interesting to analyse a 1^- state that was reported to be found at about 1.3 MeV and a width of about 0.75 MeV in a $^{11}\mathrm{Li} + p$ experiment [33]. From Table I one sees that this state lies too low to be a particle-hole excitation, since the lowest configuration of this type is $|1s_{1/2}0p_{3/2}^{-1}\rangle$ at an energy of 4.5 MeV, and it lies too high to be a particle-particle state, since the lowest two-particle configuration is $|1s_{1/2}0p_{1/2}\rangle$ at an energy of 0.215 MeV. Therefore we did not find any reasonable

TABLE IV. Pole-pole (PP), pole-continuum (PC), and continuum-continuum (CC) contributions to the s and p angular momentum content $A_l \times 100$, corresponding to the state 0_2^+ in $^{11}\mathrm{Li}$ as a function of the interaction strength G (MeV). The strength fitting the available experimental data is $G_0 = 0.1659$ MeV.

G	s content			p content		
	PP	PC	CC	PP	PC	CC
0.01	0	0	0	(100, 0)	0	0
0.05	(2, 0)	(−4, 5)	(−2, −5)	(104, 2)	(0, −2)	0
0.09	(3, 14)	(−31, −4)	(14, −22)	(101, 20)	(13, −8)	0
0.13	(−8, −3)	(8, −17)	(14, 11)	(36, 30)	(50, −21)	0
0.17	(−6, −4)	(12, −16)	(11, 16)	(39, 20)	(44, −16)	0

TABLE V. Valence single-particle states used in the calculation of the two-neutron states in ^{72}Ca. The energy E_n and the wave number k_n are related as in Eq (2). The k_n value corresponding to the state $2s_{1/2}$ shows that this is an antibound state.

State	E_n (MeV)	k_n (fm^{-1})
$2s_{1/2}$	(−0.056, 0)	(0, −0.051)
$1d_{5/2}$	(0.488, −0.053)	(0.153, −0.008)
$1d_{3/2}$	(2.089, −1.545)	(0.334, −0.110)
$0g_{7/2}$	(6.772, −0.748)	(0.568, −0.031)
$0h_{11/2}$	(5.386, −0.106)	(0.506, −0.005)

G value, even assuming a repulsive force (i.e., G real and negative) that could provide this state within our shell model approach.

B. The nucleus ^{70}Ca

We have seen in the previous subsection that in ^{11}Li(g.s.) the halo is induced by the extension of the wave functions corresponding to the valence single-particle states. This, in turn, is due to the lack of a barrier that would hold the particles tightly bound to the core. It is a delicate balance, since without the pairing interaction acting upon the valence particles the nucleus would not be bound, i.e., the ground state wave function would not be localized. One may therefore wonder whether valence single-particle states larger than $l = 1$ would still induce halos. With this aim in mind we tried to find such a case by following the trend of single-particle states in a relativistic mean-field calculation. We thus found that the nucleus ^{72}Ca (corresponding to the core $Z = 20$, $N = 50$) fulfills the conditions that we look for, since the valence single-particle states are again an antibound $2s_{1/2}$ shell but now the next shell is $2d_{5/2}$. To simulate the order of the single-particle states given by the relativistic calculations, we used a Wood-Saxon potential defined by $a = 0.67$ fm, $r_0 = 1.27$ fm, $V_0 = 39$ MeV, and $V_{so} = 22$ MeV. The corresponding single-particle states are shown in Table V. One sees that the antibound state as well as the first excited state lie near the energy threshold, as in the previous case. Even the wave function of the antibound state is similar to the one in ^{10}Li, as expected. However, since now the first excited state carries a higher angular momentum as compared with the previous case, one would expect that the corresponding wave function would be too localized, thus hindering the formation of the halo. As is seen in Fig. 10, this is not the case, since the wave function extends much beyond the standard value of the nuclear radius in ^{71}Ca, i.e., $R = 5.18$ fm.

There is another important difference between the single-particle states in Tables I and V, namely, the appearance of the narrow high-spin resonance $0h_{11/2}$. This may induce a high-lying localized two-particle resonance.

To probe the differences, if any, between ^{11}Li and ^{72}Ca, we proceeded as in the previous subsection and solved the generalized CXSM in this case by using the separable interaction provided by the field f of Ref. [8]. As already reported in Ref. [8], we thus found that the ground state two-particle wave function has the same features as the corresponding one in ^{11}Li.

There is also a second 0^+ state lying at (0.550, −0.350) MeV, which in Ref. [8] was considered to be a likely resonance. We have now the possibility of examining whether this is the case by looking at the wave function $S(r)$. The notable peculiarity of this wave function is that it looks very similar to the corresponding one in ^{11}Li, as can be seen by comparing Figs. 8 and 11. It thus seems that the nuclei ^{11}Li and ^{72}Ca are both halo nuclei, although the valence wave functions correspond to different numbers of nodes and even orbital angular momenta. This shows, once more, that the characteristic determining the formation of

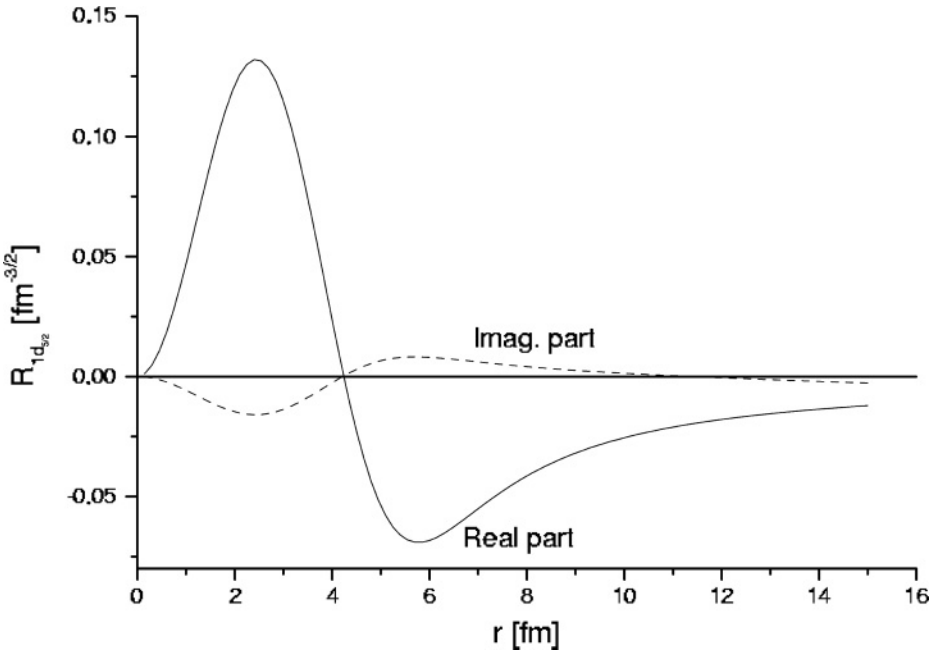

FIG. 10. Radial wave function $R_{1d_{5/2}}(r)$ corresponding to the single-particle state in Table V.

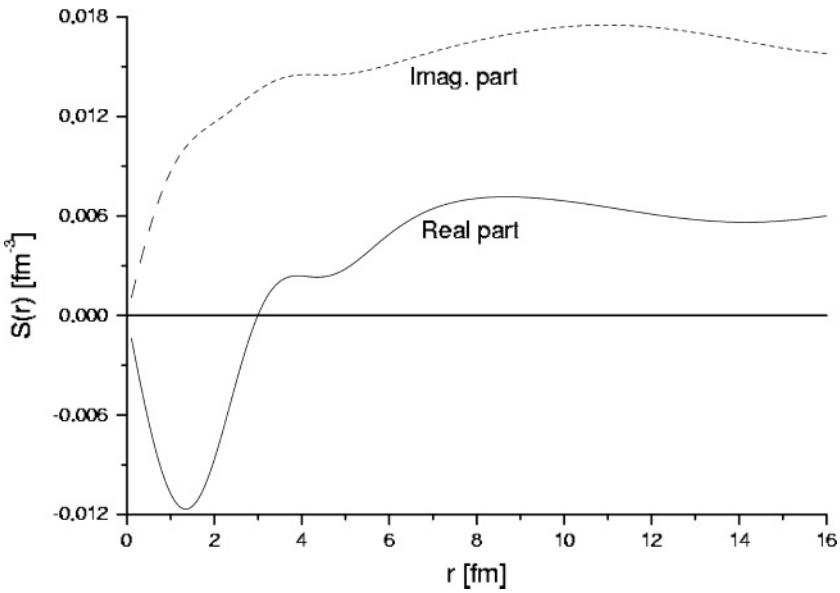

FIG. 11. Two-particle radial wave function $S(r)$ corresponding to the singlet component of the state $^{72}\mathrm{Ca}(0_2^+)$ evaluated by using the generalized Berggren representation.

halos is the extension of the valence wave functions in space, and this may happen even if the valence particles move in high-angular-momentum orbits.

We have also investigated whether a narrow two-particle resonance appears as a result of the coupling of the particles in the single-particle state $0h_{11/2}$. We did not observe this by using the strength G_0 that provides the bound ground state of ^{72}Ca. We then decided to follow the trajectory in the complex energy plane of the state $|0h_{11/2}^2\rangle$ as G increases from its zeroth-order value. As in Ref. [7] we found that this state indeed becomes narrower as G increases to a certain point, but afterwards the coupling of one of the particles to the continuum increases the width of the resonance, which eventually itself becomes part of the continuum background. We have already seen this feature above when analyzing the state 0_2^+ in ^{11}Li, and it appears again in the halo nucleus ^{72}Ca as well as in the drip-line nuclei analyzed previously by us [7]. This theory thus predicts that only if the pairing interation is relatively weak will two-particle resonances appear as the result of the coupling of the particles to high-lying narrow single-particle resonances.

IV. SUMMARY AND CONCLUSIONS

In this paper we have presented a new formalism to evaluate two-particle resonances in halo nuclei microscopically by using a generalization of the complex shell model (CXSM) presented in Ref. [7]. Since one of the elements inducing the formation of halos was found to be the appearance of antibound states lying close to the continuum threshold, this generalization consists in defining a contour in the complex energy plane that comprises the antibound states. That is, the antibound states and the Gamow states (i.e., states lying in the complex energy plane) are selected by appropiate contours in the complex energy plane. Therefore within this formalism bound states, antibound states, Gamow states, and the continuum background are all basis single-particle states treated on the same footing. These states are poles of the corresponding single-particle Green's function.

The contribution of the pole-pole, pole-continuum, and continuum-continuum configurations in the two-particle systems can be easily analyzed. The effects induced by antibound states and the continuum encircling the poles can be studied separately.

Given the rather unfamiliar characteristics of both the CXSM and the antibound states, we have described in detail those characteristics. In particular, we have shown that the effects induced by antibound states lying close to threshold on physically measurable quantities are exactly the same as those provided by bound states also lying close to threshold. In both cases the main feature is that the single-particle wave function extends far in space.

We have also analyzed the properties that a many-particle state lying on the complex energy plane may have to be considered a resonance, i.e., a measurable state appearing in the continuum part of the spectrum. We have thus found that the resonant wave function has to be localized within the nuclear system. To illustrate these features as well as to show the advantages of the formalism, we evaluated two-particle states in the well-known case of ^{11}Li as well as in the nucleus ^{72}Ca. We analyzed the localization properties of the two-particle wave functions in these nuclei, trying to find high-lying resonances. However, we did not find evidence that would indicate that such resonances exist in these cases.

Finally, we have found that the theory predicts that only if the two-body interation is relatively weak will two-particle resonances appear as the result of the coupling of the particles to high-lying narrow single-particle resonances.

ACKNOWLEDGMENTS

This work has been supported by Fondo para el mejoramiento de la calidad docente (FOMEC) and Fundación Antorcha (Argentina), by the Hungarian OTKA fund Nos. T037991 and T046791 and by the Swedish Foundation for International Cooperation in Research and Higher Education (STINT).

[1] M. V. Zhukov, B. V. Danilin, D. V. Fedorov, J. M. Bang, I. J. Thompson, and J. S. Vaagen, Phys. Rep. **231**, 151 (1993).
[2] E. Garrido, D. V. Fedorov, and A. S. Jensen, Nucl. Phys. **A700**, 117 (2002).
[3] Y. Suzuki, R. G. Lovas, K. Yabana, and K. Varga, *Structure and Reactions of Light Exotic Nuclei* (Taylor & Francis, London, 2003).
[4] J. Okolowicz *et al*., Phys. Rep. **374**, 271 (2003), and references therein.
[5] R. Id Betan, R. J. Liotta, N. Sandulescu, and T. Vertse, Phys. Rev. Lett. **89**, 042501 (2002).
[6] N. Michel, W. Nazarewicz, M. Płoszajczak, and K. Bennaceur, Phys. Rev. Lett. **89**, 042502 (2002).
[7] R. Id Betan, R. J. Liotta, N. Sandulescu, and T. Vertse, Phys. Rev. C **67**, 014322 (2003).
[8] R. Id Betan, R. J. Liotta, N. Sandulescu, and T. Vertse, Phys. Lett. **B584**, 48 (2004).
[9] G. Gamow, Z. Phys. **51**, 204 (1928).
[10] P. L. Kapur and R. Peierls, Proc. Roy. Soc. A **166**, 277 (1938).
[11] R. G. Newton, *Scattering Theory of Waves and Particles*, 2nd ed. (Springer-Verlag, New York, 1982).
[12] B. Gyarmati and T. Vertse, Nucl. Phys. **A160**, 523 (1971).
[13] T. Berggren, Nucl. Phys. **A109**, 265 (1968).
[14] R. J. Liotta, E. Maglione, N. Sandulescu, and T. Vertse, Phys. Lett. **B367**, 1 (1996).
[15] T. Vertse, P. Curutchet, and R. J. Liotta, *Proceedings of the Symposium on Resonances*, edited by E. Brãndas and N. Elander, Lecture Notes in Physics, Vol. 325 (Springer-Verlag, Berlin, 1987), p. 179.
[16] G. Breit and E. P. Wigner, Phys. Rev. **49**, 519 (1936).
[17] T. Vetse, R. J. Liotta, and E. Maglione, Nucl. Phys. **A584**, 13 (1995).
[18] T. Berggren, Phys. Lett. **B73**, 389 (1978).
[19] J. Humble and L. Rosenfeld, Nucl. Phys. **A26**, 529 (1961).
[20] V. I. Kukulin, V. M. Krasnopolsky, and J. Horacek, *Theory of Resonances* (Kluwer Academic Publishers, Dordrecht/ Boston/London, 1989).
[21] G. F. Bertsch and H. Esbensen, Ann. Phys. (New York) **209**, 327 (1991).
[22] H. Esbensen, G. F. Bertsch, and K. Hencken, Phys. Rev. C **56**, 3054 (1997).
[23] A. Bianchini, R. J. Liotta, and N. Sandulescu, Phys. Rev. C **63**, 024610 (2001).
[24] T. Vertse, P. Curutchet, R. J. Liotta, and J. Bang, Acta Phys. Hung. **65**, 305 (1989).
[25] T. Berggren and P. Lind, Phys. Rev. C **47**, 768 (1993).
[26] L. Gr. Ixaru, *Numerical Methods for Differential Equations* (Reidel, Dordrecht, 1984); L. Gr. Ixaru, M. Rizea, and T. Vertse, Comput. Phys. Commun. **85**, 217 (1995).
[27] I. J. Thompson and M. V. Zhukov, Phys. Rev. C **49**, 1904 (1994).
[28] H. G. Bohlen *et al*., Nucl. Phys. **A616**, 254c (1997).
[29] A. B. Migdal, A. M. Perelomov, and V. S. Popov, Yad. Fiz. **14**, 874 (1971) (in Russian); Sov. J. Nucl. Phys. **14**, 488 (1972).
[30] R. G. Lovas, R. J. Liotta, A. Insolia, K. Varga, and D. S. Delion, Phys. Rep. **294**, 265 (1998).
[31] T. Vertse, A. T. Kruppa, R. J. Liotta, W. Nazarewicz, N. Sandulescu, and T. R. Werner, Phys. Rev. C **57**, 3089 (1998).
[32] F. A. Janouch and R. J. Liotta, Phys. Rev. C **27**, 896 (1983).
[33] A. A. Korsheninnikov *et al*., Phys. Rev. Lett. **78**, 2317 (1997).